Earth and Planetary Science Letters 292 (2010) 68–78

Contents lists available at ScienceDirect

Earth and Planetary Science Letters

journal homepage: www.elsevier.com/locate/epsl

How much magma is required to rift a continent?

Robert W. Bialas *, W. Roger Buck, Ran Qin

Lamont Doherty Earth Observatory, 61 Route 9W, Palisades, NY 10964, United States

ARTICLE INFO

Article history:
Received 15 June 2009
Received in revised form 5 January 2010
Accepted 16 January 2010
Available online 11 February 2010

Editor: Y. Ricard

Keywords:
rifting
magma
continental Breakup
diking

ABSTRACT

Many continental rifts are associated with and preceded by the formation of large igneous provinces. Partial melting of a large region of anomalously hot, upwelling mantle is required to explain these huge volumes of pre- and syn-rift basaltic magma. The uplift associated with a shallow region of hot mantle is often invoked as a cause of the "rift-push" force that may drive the observed extension. The rift-push force is likely to be an order of magnitude too small to drive tectonic stretching of normal continental lithosphere, but may be sufficient to drive opening of lithosphere-cutting dikes. Intrusion of a sequence of such dikes along a narrow zone may provide enough heat to significantly weaken the lithosphere. Here we use a newly developed 2D numerical approach, in which magma filled dikes open in continental lithosphere in response to an evolving model stress field, and the advection and diffusion of heat is tracked, to investigate the relation between the volume of magma and the amount of lithospheric weakening. The available rifting force, lithospheric structure, and parameters controlling magma flux are varied in the numerical simulations. For continental lithosphere ≥60 km thick ($H_L = H_{1200\,°C}$) heat diffusion is unimportant and only a small amount of magma is required (<4 km of maximum cumulative dike opening) to weaken the lithosphere such that it may rift without additional magma. The volume of magma per unit length of rift required to transition from magmatic to tectonic rifting using our method is less than half of that reported by an earlier study. For reasonable plate-tectonic time scales, the amount of magma required for this transition is nearly independent of the rate of magmatic injection, with the exception of highly extrusive cases. Thus, magma assisted rifts may transition to tectonic rifts with rapid magma injection over a short period of time (~1 m.y. as seen for some "volcanic margins" like the North Atlantic) or with slow rates over longer time scales (>10–20 m.y. similar to "magmatic rifts" like the Red Sea).

1. Introduction

Most continental-scale rifts that proceed to sea floor spreading develop in association with large igneous provinces (LIPs) (Hinz, 1981; Hill, 1991), during which magma may erupt for more than 10 Ma, but most of the volume is erupted over a period of one million years or less (Courtillot and Renne, 2003; Wolfenden et al., 2004, 2005). Despite the correlation between magmatic events and continental breakup, many models of continental breakup ignore the importance of magmatism and dike intrusion in rift evolution (e.g., McKenzie, 1978; Royden and Keen, 1980; Braun and Beaumont, 1989; Buck, 1991; Davis and Kusznir, 2004), or have focused on magma generated due to asthenospheric upwelling in response to lithospheric stretching (e.g., White and McKenzie, 1989; van Wijk et al., 2001; Nielsen and Hopper, 2002). However, magmatism associated with LIPs often precedes rifting, including in the Red Sea (Bosworth et al., 2005), North and South Atlantic rifts (Courtillot et al., 1999; Courtillot and Renne, 2003 and refs. therein). The giant dike swarms that precede continental breakup may require a major thermal perturbation in the upper mantle (e.g., Fialko and Rubin, 1999). Our model is not sensitive to whether pre-rift magma is generated via plumes (LeCheminant and Heaman, 1989; Hill, 1991) or other mechanisms, such as super-continent insulation (Coltice et al., 2009).

Dike intrusions in continental rifts associated with LIPs can be 10s to 100s of meters wide and several thousand kilometers long (Fahrig, 1987; Ernst and Buchan, 1997). Extensional tectonic force is required to open such dikes, but this force is much less than that needed to produce amagmatic stretching via normal faulting (e.g., Buck, 2004). In addition to adequate force levels, sufficient magma flux is necessary to open dikes and sustain magmatic rifting (Buck, 2006; Qin and Buck, 2008).

Whether dike intrusions lead to continental rifting and breakup may depend on how much magma is intruded into a region. Intrusion of hot basaltic magma in dikes will heat and weaken the lithosphere (e.g., Royden et al., 1980). With sufficient weakening, rifting should continue even if the supply of magma wanes or ends. Estimating the amount of magma needed to weaken the lithosphere has been done in other studies that treat kinematic dike opening. Buck (2004) treated steady opening of dikes in a numerical model of the thermal evolution of a rift, but he could only make a rough estimate of the mechanical effect of lateral change in thermal structure on the strength of a rift. Dikes have been treated in a fully visco-elastic-plastic code by accreting frozen magma at a preset spreading center as some percentage of extension,

* Corresponding author. Lamont Doherty Earth Observatory, 61 Route 9W, Palisades, NY 10964, United States. Tel.: +1 201 264 0776; fax: +1 845 365 8156.
E-mail address: rbialas@ldeo.columbia.edu (R.W. Bialas).

0012-821X/$ – see front matter © 2010 Elsevier B.V. All rights reserved.
doi:10.1016/j.epsl.2010.01.021

called the *M*-factor (Buck et al., 2005). Behn et al. (2009) used this *M*-factor approach to estimate magma volumes, but this approach emplaces dikes with preset dimensions without regard for the local stress field or regional extensional forces.

Herein, we seek to provide a mechanically consistent treatment of dike opening and heat emplacement as rift lithospheric strength evolves. Our goal is to more precisely estimate the amount of magmatic dike opening and the magma injection rate required to weaken the lithosphere such that it may rift on its own, without further dike injection. Real rifts involve complications such as pre-existing weaknesses and variable rates of magma input that are not treated herein, but our idealized models, which are the most complete to date, allow us to gain insight into the physical processes occurring in real magmatic rifts.

We investigate the effects of repeated dike intrusions into a 2D region of continental lithosphere using an approach that estimates opening for each dike. This is done by computing the stress distribution before and after the dike intrusion for set parameters of available magma supply and pressure. We explore how changes in the stress field affect magma distribution in space and time, focusing on the influence of the rate of magma injection versus thermal diffusion on the amount of magma input required before such a region can tectonically rift, that is rift with the available tectonic force without additional magma. Lastly, we examine the maximum thickness lithosphere that may be able to undergo rifting with the assistance of dike injection and discuss possible real world applications.

2. Conceptual model

Dikes open in response to lithospheric stress. Because intruding dikes have nearly the same density as the crustal host rock (Fig. 1a and b), the stress difference needed to open dikes can be substantially less than that needed for tectonic extensional normal faulting (Fig. 1c and d) (Buck, 2006; Qin and Buck, 2008). Since we are concerned with extension of the entire lithosphere, we consider the vertically integrated stress, or force per length, of a rift. In situations where the force for rifting is derived from uplift of the lithosphere over abnormally hot mantle (Spohn and Schubert, 1982; Bott, 1991), the available rifting force is roughly equivalent to that of ridge push (Bott, 1991). If the lithosphere is initially thin (and so weak) or the extensional force is very large, then little or no magma weakening should be needed to a allow rifting to proceed. For continental lithosphere with a normal heat flow (~40–50 mW m^{-2}) and crustal thickness, H_C, ~40 km, the lithosphere should be close to 80 km thick (Turcotte and Schubert, 2002), and the ridge push force is likely not large enough to drive tectonic rifting, but it is large enough to open dikes (Fig. 1e) (Buck, 2004, 2006).

Dikes are magma filled cracks in the lithosphere, thus we have to treat the elastic behavior of dike opening. Since we are concerned with the temperature controlled strength of the lithosphere through time, we also have to track the viscosity of the crust and mantle. Though we are interested in force levels that may be too low to form lithosphere-cutting faults, enough force may be present to fault the brittle crust above the dike. Fault strain is simulated with a plastic (yield stress limited) rheology. Thus, a visco-elastic-plastic rheology is used to model the lithosphere.

In this paper we estimate the amount of magma required to sufficiently weaken the lithosphere to the point that rifting can continue without continued magmatic input. Thus, we look at the evolution of lithospheric strength in models with different values of 3 variables: lithospheric thickness (H_L), available extensional force (F_A)

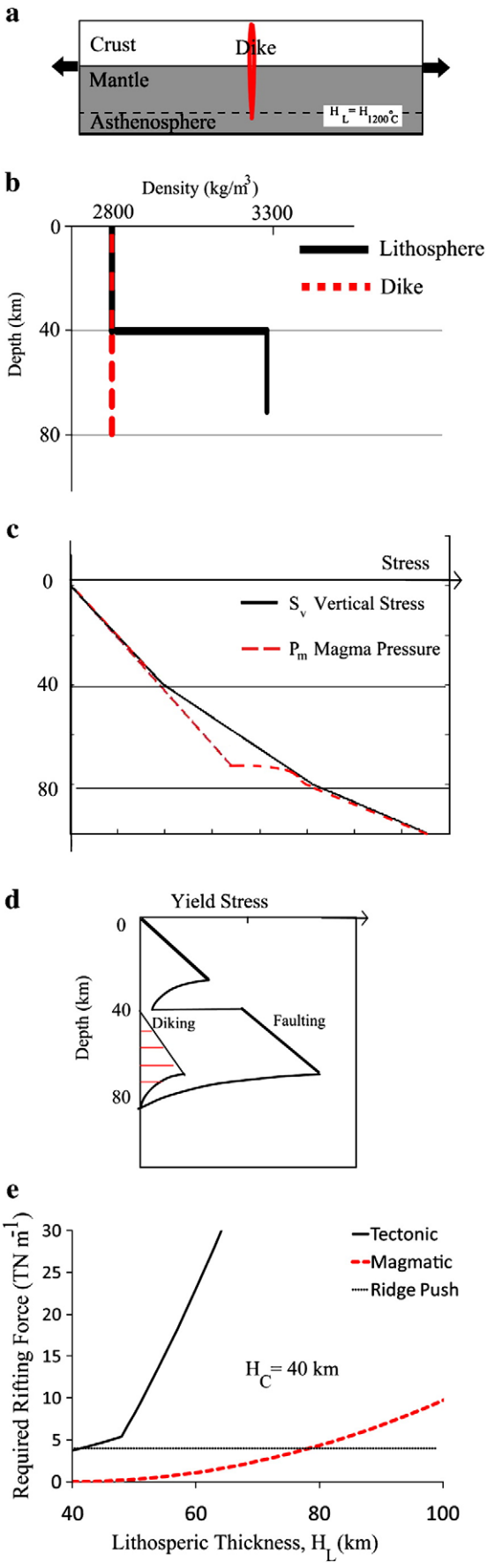

Fig. 1. (a) Lithospheric structure. (b) Density profile of lithosphere and diking column with depth. (c) Stress profile of lithosphere and dike with depth. (d) Yield stress for faulting versus dike emplacement. (e) Force required to rift versus lithospheric thickness. For the magmatic case, crustal thickness is 40 km, and magma fills dikes up to the surface. The tectonic force is estimated following Buck (2006) but is under-estimated by assuming strength in the crust only though 300 °C and in the mantle through 1000 °C, neglecting strength in ductile zones.

and magma flux. Of these the magma flux is the most difficult for us to specify directly in the context of our simulation of dike opening. The amount of magma intruded in an event depends on the lithospheric stress and the magma pressure. Computing the lithospheric stress is straightforward, as described below, but specifying the magma pressure is harder. For example, were we to fix a magma pressure that was sufficient to allow extrusion, then the amount of extrusion would be unlimited. We chose to assume that as more magma is intruded into a region the magma pressure is reduced. This assumption is based on observations of active dike events in places like Hawaii and Iceland where source regions are seen to subside during the short time when dikes are seen to open (Tryggvason, 1984; Einarsson, 1991; Segall et al., 2001). It appears that the source region and the dike form a "closed-system" during a dike event. The withdrawal of magma from a "magma chamber" source region surrounded by elastic rocks should result in a reduction in pressure and the pressure drop should increase with the magma volume removed. We assume that the magma at the start of an event has a given pressure (P_0) and that the pressure is linearly reduced with the volume intruded into dikes.

3. Description of hybrid kinematic, dynamic boundary condition

In order to model a force-limited rift, we impose a hybrid boundary condition that combines aspects of kinematic and dynamic conditions. We pull on the sides of a block of lithosphere at a set velocity until the force difference reaches a set maximum value (Fig. 2a), at which time we stop pulling (Fig. 2b). Dikes periodically injected into the center of the model domain reduce elastic stresses and so decrease the force difference (Fig. 2b). When the force difference is reduced by an arbitrary amount, by diking and/or viscous relaxation, we resume pulling on the sides of the model (Fig. 2c). With repeated intrusions, enough heat enters the system to locally weaken the lithosphere such that it may rift on its own without the injection of additional magma (Fig. 2d). We dub this time the onset of tectonic rifting.

Before extension, the horizontal stress, S_h, at any depth, z, equals the vertical, lithostatic stress, S_v:

$$S_v(z) = g\int \rho(z)dz \tag{1}$$

where g is gravitational acceleration, 9.8 m s^{-2}; $\rho(z)$ is the density, in our case a crustal layer with $\rho_c = 2750$ kg m^{-3} overlying a mantle layer with $\rho_m = 3300$ kg m^{-3} (Fig. 1b); and z is the depth (Turcotte and Schubert, 2002; Qin and Buck, 2008). Extension of the elastic lithosphere reduces S_h tectonically by some amount, S_d, such that:

$$S_h(z) = S_v(z) - S_d(z) \tag{2}$$

To simulate extension with a limited extensional force, we start with a lithostatic stress state and pull the sides of the model lithosphere at a

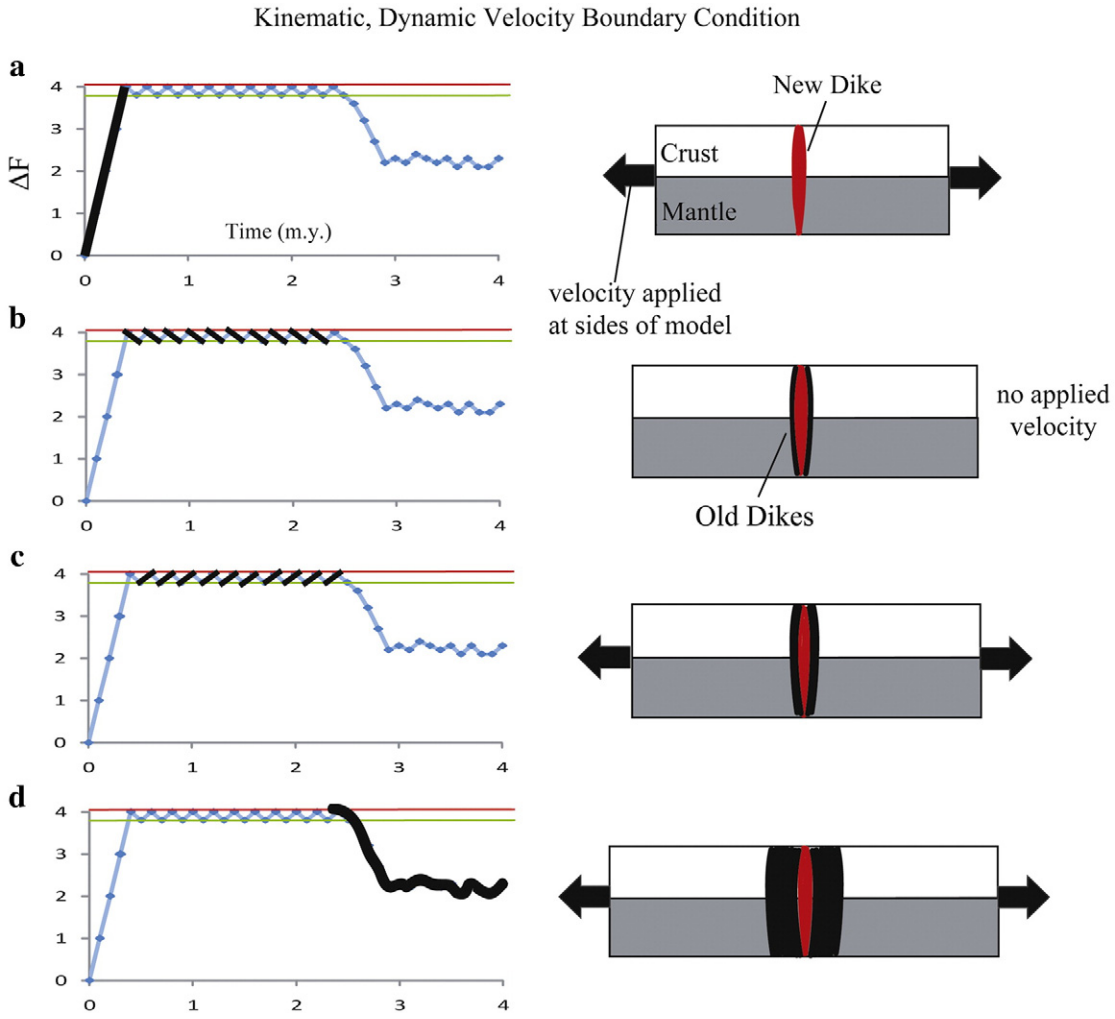

Fig. 2. Cartoon plot and diagram illustrating the kinematic–dynamic boundary condition. Darkened sections of the ΔF plot correspond to the lithospheric state at right. At the model's inception, the force difference is below the available rifting force (red line), and a velocity is applied to the sides of the model (a). With extension, ΔF increases until it equals the rifting force (a), and the applied velocity is set to 0 (b). Diking continues, decreasing ΔF (b), and the velocity is reset (c). For numerical reasons, we must apply a finite force drop (green line) before restarting the velocity. This cycle repeats until the model is weak enough to extend unhindered (d).

constant velocity (Fig. 2) such that S_h is reduced by S_d. The resulting force difference is:

$$\Delta F = \int S_d(z)dz. \quad (3)$$

Throughout model time, diking occurs at the center of the model at a periodic interval, relieving S_d and decreasing ΔF. When extension increases ΔF such that it is greater than the force available for rifting, F_A, (when i.e. $\Delta F \geq F_A$) we stop pulling on the model (Fig. 2b). While pulling is stalled, diking and viscous relaxation decrease ΔF until $\Delta F < F_A$, at which time extension resumes (Fig. 2c). We must assume a finite, but small, drop in force before restarting extension (Fig. 2, green line). Varying this force drop between 1% and 20% of F_A did not significantly affect the results.

Dike opening accretes material to the center of the model at 1200 °C, and additional heat enters the system due to the latent heat of dike solidification. The viscosity of the crust and the mantle is temperature dependent, scaling as:

$$\mu \propto e^{E_a / nrT} \quad (4)$$

where E_a is the activation energy, n is the power law exponent, r is the gas constant, and T is the temperature (Kirby and Kronenberg, 1987). With enough heat injection, the lithosphere weakens such that ΔF stabilizes at or below F_A (Fig. 2d), signaling the onset of tectonic rifting. Though diking may continue, it is no longer required to continue rifting. Relating the thermal weakening associated with diking to the extensional force requires a numerical model.

4. Numerical methods

We examine the effect of dike intrusion into a section of lithosphere using highly-idealized, regional scale, two-dimensional numerical models. The simplified lithosphere is a 640 km wide box consisting of a layer of crust overlying a layer of mantle. The crust has a dry plagioclase rheology with $\rho_{crust} = 2750$ kg m^{-3}, $E_a = 238$ kJ mol^{-1}, and thermal conductivity $= 2$ Wm^{-1} K^{-1}. The mantle is modeled with an olivine power law creep rheology with $\rho_{mantle} = 3300$ kg m^{-3}, $E_a =$ 511 kJ mol^{-1}, and thermal conductivity $= 3$ Wm^{-1} K^{-1} (Table 1) (Kirby and Kronenberg, 1987). The initial thermal profile is defined by a linear thermal gradient to a bottom temperature of 1200 °C. There is no initial thermal perturbation in the model. Our conceptual dikes are sourced at some distance from the modeled cross section (Fig. 3). Our modeled section of lithosphere is a cross section perpendicular to the radiating direction of the dikes (Fig. 3).

Table 1
Simulation variables and constants.

Variable		Standard case	Range in models
Diking terms			
H_C	Crustal thickness	40 km	14–40 km
H_L, $H_{1200\ °C}$	Lithospheric thickness	80 km	20–120 km
v_A	Applied half velocity	0.5 cm yr^{-1}	0.5 cm yr^{-1}
F_A	Extensional force	4.2 TN m^{-1}	1–4.2 TN m^{-1}
D_I	Diking interval	5000 yrs	5000 yrs
MCE	Magma chamber efficiency	Varied	10^{-1}–10^{-4} m^2 Pa^{-1}
h_{ph}	Magma pressure head	Varied	100–10,000 m
Rheology terms (crust, mantle)			
ρ	Density	2750, 3300 kg m^{-3}	
k	Thermal conductivity	2, 3 W m^{-1} K^{-1}	
n	Non-Newtonian power law exponent	3.2, 3	
r	Gas constant	8.31 J mol^{-1} K^{-1}	
E_a	Activation energy	238, 511 kJ mol^{-1}	
A	Pre-exponential of the effective viscosity	3.2×10^{-4}, 7×10^{4} MPa^{-n}	

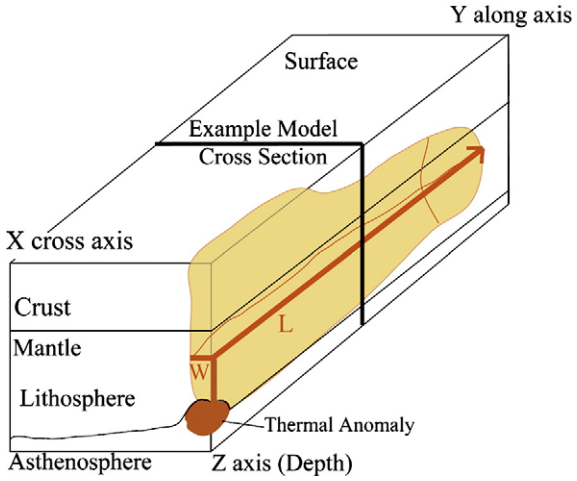

Fig. 3. Schematic view of large dike intrusion into continental lithosphere. A magma chamber above a thermal anomaly radiates dikes hundreds to thousands of kilometers from a central source. We show an example location for our 2D model cross sections.

Deformation is tracked using an explicit finite difference method similar to the FLAC (Fast Lagrangian Analysis of Continua) technique (Cundall, 1989). It has previously been used to investigate local deformation (e.g., Lavier et al., 2000) and regional deformation (e.g., Bialas et al., 2007). Brittle behavior is modeled using Mohr–Coulomb criterion for elasto-plasticity (with a friction coefficient of 0.6 and an initial cohesion of 20 MPa), and viscous behavior is modeled by a non-Newtonian viscosity based on power law creep (Kirby and Kronenberg, 1987). A small amount of strain weakening is applied such that cohesion decreases from 20 to 14 MPa between plastic strain values of 0 to 1. Grid spacing is ~2 or ~4 km, and remeshing is triggered in areas of very large deformation. Altering grid size from 2 to 4 km does not affect the results. A complete description of the finite difference method can be found in Lavier et al. (2000) and Bialas et al. (2007).

In order to simulate diking, we employ a boundary element method based on TWODD (Two-dimensional displacement discontinuity method) (Crouch and Starfield, 1983) to calculate the deformation of a dike in a non-gravitational half-space. Such a method is appropriate as long as the along-axis dike length is several times larger than its height. A major advantage over previous studies is the dike top and bottom, in addition to the width, are calculated using Weertman's method (Weertman, 1971), rather than arbitrarily assigning a dike height at the start of the problem as many previous models of dike emplacement have done (e.g., Rubin and Pollard, 1987; Rubin, 1990). This approach has been previously used to investigate dike width (Qin and Buck, 2008) and morphology (Qin, 2008) at mid ocean ridges.

Because dike opening, magma volume, and pressure on the dike wall are linked, we numerically iterate to solve for the dike opening (Qin and Buck, 2008) (further explained in Appendix A). We ignore magma flow related stress variations during dike opening. Thus, the equilibrium condition at the wall of a dike is that the magma pressure, $P_m = S_h$. At any depth $P_m(z)$ is calculated as the pressure at a reference depth plus the static variation with gravity

$$P_m = P_0 + g\rho_m z \quad (5)$$

where P_0 is the magma pressure at the surface ($z = 0$) and ρ_m is the density of the magma in the dike, $\rho_m = 2750$ kg m^{-3} (Fig. 1b and c).

Dikes are injected at a preset, regular diking interval, D_I, inspired by historical observations, e.g. the Krafla segment of Iceland (Saemundsson, 1979). While ideally the timing of dike injection would be self-determining based on the stress field and magma supply, such a technique is not feasible in our numerical approach at this time. The time interval for diking, D_I, must be chosen. The D_I can affect dike size if the stress field is changing during that time interval. For our

kinematic–dynamic boundary condition, if ΔF is at its maximum, a longer D_I will not affect dike size as no additional stresses build during the additional time. However, a larger D_I will result in large dikes if ΔF increases during the expanded diking interval. For our numerical approach, D_I must be at least a few time steps to allow for the FLAC code to update between diking events. For the models herein, $D_I = 5000$ yrs, with FLAC time steps averaging 0.5 yrs, well within our limitation. While the timing of individual dikes in large continental dike swarms is poorly constrained, our chosen D_I results in the observed range of dike size and allows us to investigate a wide range of magma supply rates.

A single dike is calculated per event. Dike swarms or repeat injections are not treated. Modeled dikes are always vertical and intrude at the model's centerline. Each dike is initiated at a preset isotherm (in most cases presented, the 700 °C isotherm), and the dike is initially ~1 km in height. The dike is allowed to grow both upwards and downwards at the same velocity until each tip stops opening. An intrusion event is assumed to be fast enough that we can neglect magma freezing during the dike event, but slow enough that viscous flow can be ignored. Resistance to opening at the dike tip is ignored, assuming zero fracture toughness. In the event of zero opening during a diking event, there is no update to the stress field. If a dike cracks the surface with enough pressure, extrusion, modeled as a series of layered flows that increase surface topography with crustal material, occurs.

As a dike propagates, more magma is removed from the hypothetical source region, reducing the magma pressure within the source region and at the dike wall. The source region is treated as a Mogi source (Mogi, 1958), and the magma volume per length of rift, ΔV_m, that can be pulled out at a given magma pressure change can be written as:

$$\Delta V_m = \frac{3\pi R^2}{4\mu}\Delta P \tag{6}$$

where R is the radius of a cylindrical source region, μ is the shear modulus of the source region, and ΔP is the difference between the magma pressure in the source region before and after dike intrusion. Reorganizing,

$$\mathrm{MCE} = {}^{\Delta V_m}\Big/_{\Delta P} = \frac{3\pi R^2}{4\mu} \tag{7}$$

we refer to the ratio: $\Delta V_m/\Delta P$ as the magma chamber efficiency (MCE) ($m^2\ Pa^{-1}$) and set this value at the beginning of each simulation, as the volume of source material is important in determining dike size and length in natural systems (Fialko and Rubin, 1999; Qin and Buck, 2008). Altering the MCE between simulations is equivalent to changing the size of the initial magma chamber by changing R.

The magma pressure in the model dike varies with depth as in a static fluid column with magma density, ρ_m, and the initial surface pressure, $P_0 = \rho_m g h_{ph} - \Delta P$, which is also set at the start of each simulation in terms of pressure head, h_{ph}, the maximum supported height above the initial model surface for that column (Table 1).

The FLAC and TWODD codes work in tandem to model the effects of dike intrusions in the lithosphere. FLAC simulates the steady changes in stress, viscous flow, and faulting. When a diking event is triggered, TWODD uses the information from FLAC to calculate stress changes and displacements from the dike intrusion. This information is interpolated back into the finite difference mesh of FLAC. A dike calculated in TWODD is inputted into FLAC in its "frozen" state with the same diabase rheology as the crust. As dikes are 1–10 m wide and grid elements are 2 or 4 km wide, using the same rheology for crust and dikes avoids numerical problems in the crust, where most of the dike opening occurs. In the mantle, there is some mixing of rheologies. The dominant rheology is used in model calculations, but a weighted average is used to calculate the element density.

Advection and diffusion of heat are tracked in FLAC since temperature changes affect the rheology. The concentration of radiogenic elements is set to 0 $\mu W\ m^{-3}$. While continental lithosphere certainly contains radiogenic elements, removing this complication from our models allows us to isolate and investigate the thermal effects of diking. When TWODD calculates a dike, the newly accreted material enters at 1200 °C and adds the latent heat of solidification to the system. The heat input from the dike calculated in TWODD is interpolated back into FLAC, which updates the temperature field. The viscosity updates as a result of the temperature change, and the rheology is updated to include the accreted crustal material.

5. Results

The results presented herein are for a section of continental lithosphere of normal thickness, $H_L = H_{1200\ °C} = 80$ km, modeled as 40 km of crust overlying 40 km of mantle. Altered model parameters are the MCE and h_{ph}. F_A, the available extensional force (maximum allowed ΔF), is 4.2 TN m^{-1}. Models with varied lithospheric architecture and rifting force are treated in the discussion.

Chronologically, models are split into 2 periods: the magmatically assisted phase, during which the lithosphere cannot extend without further magmatic input, and the tectonic phase, when the lithosphere has sufficiently weakened to extend with or without the input of additional magma. All models begin in the magmatic phase, but not all transition to tectonic rifting.

5.1. Example model

Fig. 4 presents time slices of lithosphere structure, temperature, viscosity, and topography for an example model with MCE = $10^{-3}\ m^2\ Pa^{-1}$ and $h_{ph} = 1$ km. At 1 m.y., the lithosphere has extended ~2 km, and the maximum cumulative dike opening is ~0.85 km at a depth of 25 km (Fig. 5b). Faulting in the upper crust forms rift flanks peaking at ~200 m. The thermal perturbation created by diking is visible as a narrow spike in the temperature profile and a decrease in viscosity of the lower crust and upper mantle.

At 2 m.y., the lithosphere has extended ~4.2 km; the extension rate has increased due to the weakening. Between 1 and 2 m.y., the majority of dike opening has occurred in the crust. Continued diking has further raised isotherms, and diffusion has extended the width of the thermal perturbation. The weak region, heated by the dikes, has a viscosity of 10^{20} to 10^{21} and extends almost the entire height of the lithosphere. The rift flanks have decreased in height slightly due to the increased percentage of extension accommodated by dike opening in the upper crust, and a deep fissure has developed above the dike.

The model transitions to tectonic rifting after 2.6 m.y. and 7.6 km of magma assisted rifting. As the model nears the transition, the extension rate increases further due to weakening, and the maximum velocity of 0.5 cm yr^{-1} is applied to each model side after the transition. Between 2 and 2.6 m.y., there is no additional dike opening in the mantle as the mantle portion of the diking zone has begun to deform ductily due to the thermal weakening. The colder crust requires more heat input to weaken, and maximum cumulative dike width is ~3.9 km at a depth of ~15 km (Fig. 5b). Viscosities are on the order of 10^{19} Pa s in the diking zone.

Two additional time slices at 5 and 9 m.y., during the tectonic rifting phase, are shown. In this example, diking continues but is not required to sustain rifting. Dike opening is outpaced by extension at the sides of the model. The crust begins to significantly thin, and a deep basin is formed. Mantle material at 1200 °C is pulled up with continued stretching.

5.2. Results with varied model parameters

In models with combinations of high MCEs and h_{ph}s, dikes are large, penetrating the entire lithosphere (Fig. 5c), and extrusion occurs, increasing surface topography and adding a load to the lithosphere

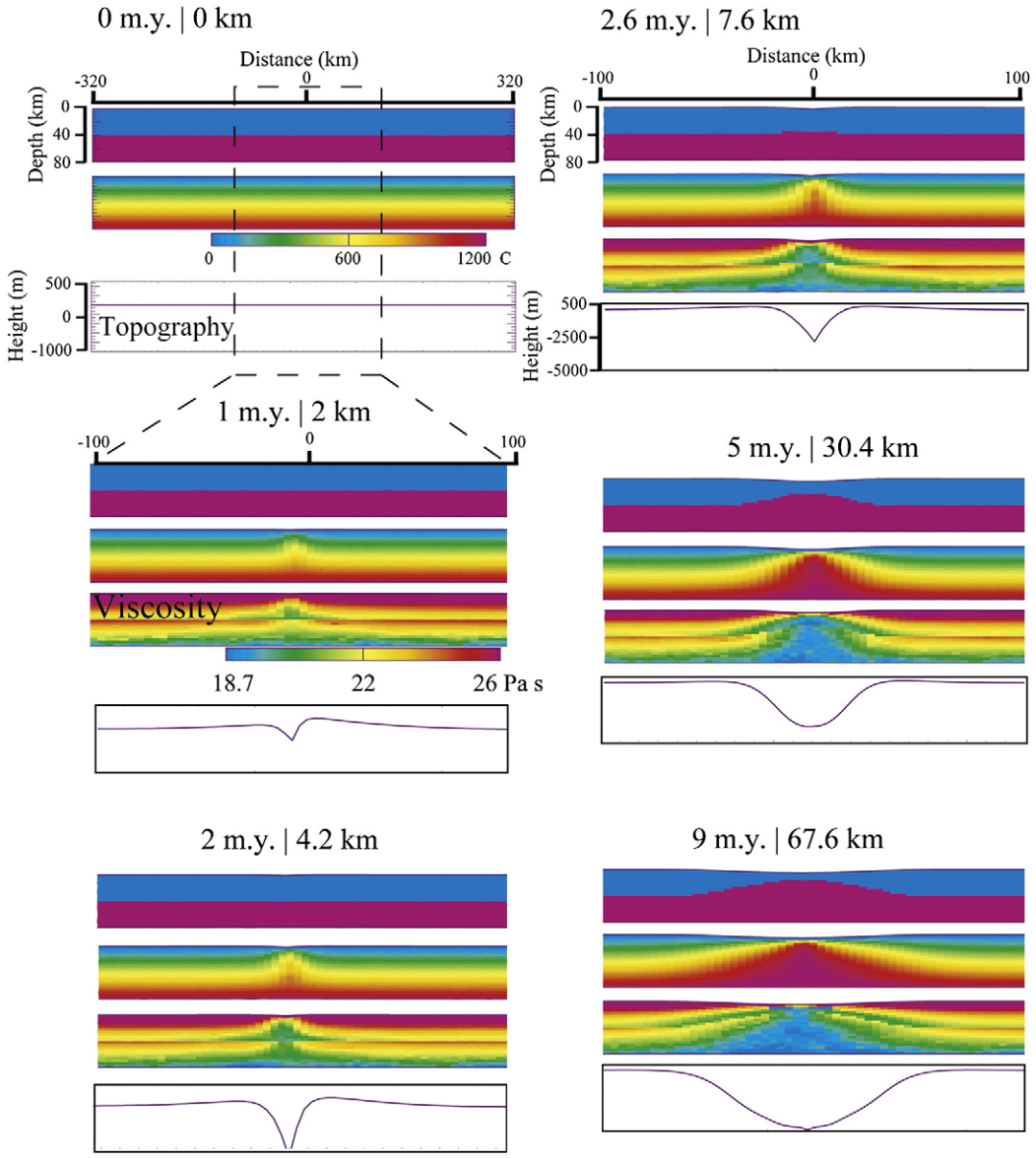

Fig. 4. Time slices for an example model with $H_L = H_{1200\ °C} = 80$ km, MCE $= 1 \times 10^{-3}$ m^2 Pa^{-1}, $h_{ph} = 1$ km, and $F_A = 4.2$ TN m^{-1}. Initially, isotherms and surface topography are flat. After 1 m.y., isotherms have been raised in the area of diking, and rift flanks ~200 m high have formed. Between 1 and 2 m.y. the extension rate has increased, and isotherms have been further raised, lowering the viscosity of the diking zone by 1–2 orders of magnitude. At $t = 2.6$ m.y., the model transitions to a tectonic rift. The basin has deepened but rift flanks have remained at ~200 m. Through 5 and 9 m.y., the model extends at 0.5 cm yr^{-1} per side, and hot mantle material is pulled up from below.

(Fig. 6a, green). The height of the volcanics increases with increased magma input parameters to a maximum of h_{ph}. Isotherms are raised in a narrow area prior to the transition (Fig. 6b), and the high heat fluxes reduce the time to tectonic rifting compared to models with slower magma input rates (Fig. 7). The load from the extrusives also influences the extensional system by increasing the vertical stress, S_v, effectively decreasing ΔF (Fig. 6c). If the extrusive load is large enough, ΔF will be depressed such that it never reaches F_A, and the system will continuously extend. This loading effect reduces the time to and amount of magma required for the transition to tectonic rifting.

Comparatively, models with low rates of magmatic input have smaller, narrower dikes (Fig. 5a) and require more time to transition to tectonic rifts (Fig. 7). Dike opening in these slower models is initially concentrated in the mantle until enough heat is injected to significantly raise isotherms (Fig. 5). The lack of magmatic extension in the upper crust during the first few million years leads to more faulting, creating higher rift flanks and deeper basins than more magmatic models (Fig. 6a). Isotherms are raised across a broader area than cases with higher magmatic input (Fig. 6b) due to the longer transition time.

Fig. 7a shows the effects of altering MCE and h_{ph} on the time to transition to tectonic rift. Models with high MCE and h_{ph} transition to tectonic rifting almost immediately, in part due to the loading effect from extrusives. For steady h_{ph} and decreasing MCE or steady MCE and decreasing h_{ph}, the time required to transition to tectonic rifting is lengthened.

Varying MCE and h_{ph}, along with all factors affecting dike size (Table 1), will vary the magma injection rate, $\dot{\boldsymbol{m}}$ = (magma to tectonic rifting)/(time to tectonic rifting) (m^2 m.y.$^{-1}$). While $\dot{\boldsymbol{m}}$ ignores changes in magma distribution with depth, using this approximation for the average magma flux allows us to distill MCE, h_{ph}, and D_l to a single term. Models with the same F_A, H_C, and H_L with similar $\dot{\boldsymbol{m}}$ require similar amounts of time to transition to tectonic rifting, regardless of the combination of MCE, h_{ph}, and D_l (Fig. 7b). This transition time increases as a power law function with $\dot{\boldsymbol{m}}$, as it is a function of time vs. rate: t = magma(t)/t. If the amount of magma input is constant with time,

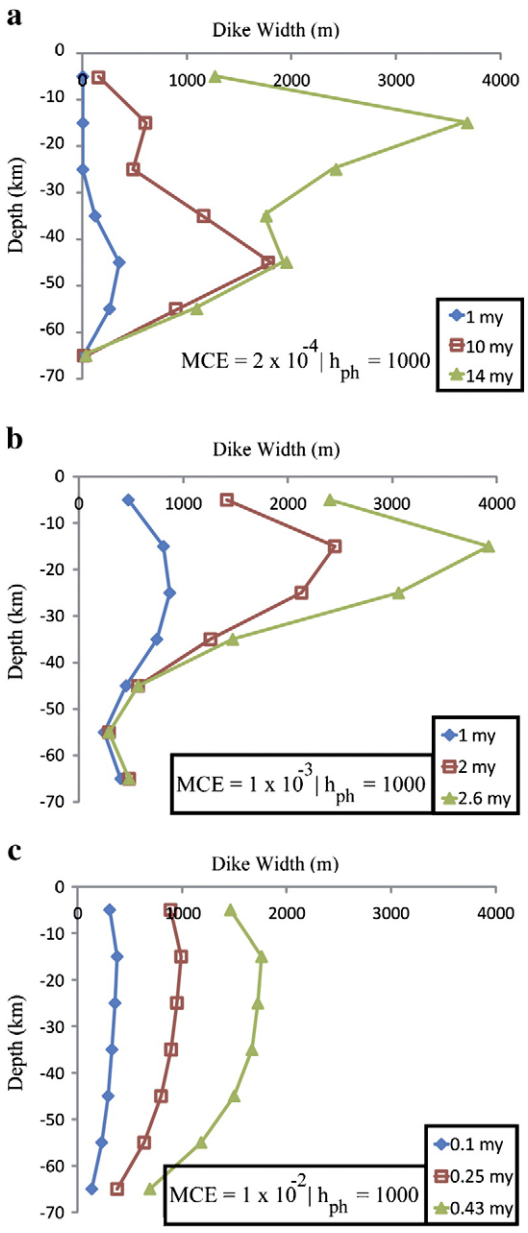

Fig. 5. Cumulative dike opening (m) is plotted against depth (km) at different time intervals for 3 models with varied MCE, $h_{ph}=1$ km, $H_L=80$ km, and $F_A=4.2$ TN m^{-1}. The latest time interval shown is the time at which the model transitions to tectonic rifting. Plot (b) is the case presented in Fig. 4. For high MCE dikes are large and have a consistent blade like shape through the lithosphere. With decreasing MCE, the distribution of magma is uneven. For low to medium MCE, dikes first open in and weaken the mantle before intruding the crust. Maximum dike opening is similar (~4 km) for cases that transition at 2.6 m.y. and 14 m.y.

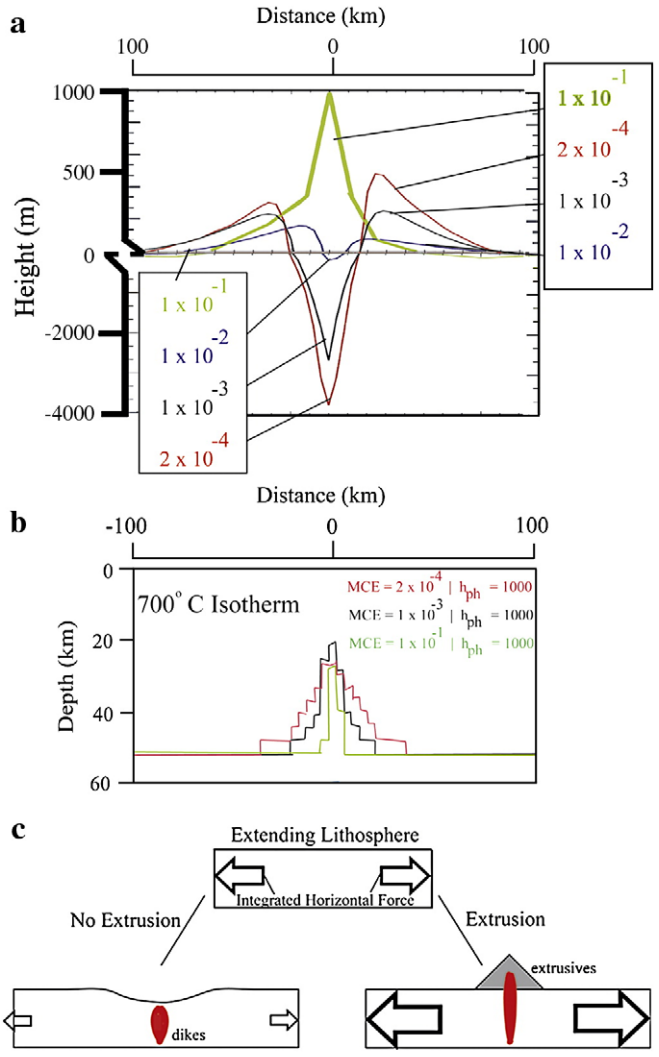

Fig. 6. (a) Topography at the time of the transition to tectonic rifting for models with $h_{ph}=1$ km, $H_L=80$ km, and $F_A=4.2$ TN m^{-1}. Note the different scales for top and bottom panels. High MCE, h_{ph}, or combinations of each produce high piles of extrusives. Low values produce deep basins and high rift flanks. Rift flank height increases, and basins deepen with decreasing MCE. (b) Plots of the 700 °C isotherm at the transition time to tectonic rifting for 3 of the above models. The height reached by the isotherm is similar across all cases, but the width of the thermal perturbation increases with decreasing magma supply and pressure. (c) Cartoon illustrating the effects of extrusion on the integrated vertical force. The extrusive load increases this force, which effectively decreases ΔF.

the slope of this power law function equals −1, as the function takes the form: $t=$ constant/t. The more negative the slope of the power law function, the more magma is required with increasing time to tectonic rifting. For the above cases, only a small increase in the area of magma needed to transition is required with increasing time to tectonic rifting (Fig. 7c). Cases with high $\dot{m}$ are affected by extrusive loads ($\dot{m} > 10^8$ m^2 m.y.$^{-1}$) and require less magma than expected (Figs. 6c and 7c).

6. Discussion

Our numerical approach is the first to investigate the long term thermal and strength evolution of rifting lithosphere cut by a series of magma filled dikes resulting from the stresses acting on the dike walls. While these stresses, the lithospheric structure, and the available extensional force affect dike dimensions, the MCE, h_{ph} , and D_I are the only parameters whose sole function is related to diking. By varying combinations of these parameters, we are able to vary the magma flux for a section of lithosphere under different condition and reproduce a wide range of model behaviors.

6.1. How much magma do we really need?

The total width of dike opening required to transition to tectonic rifting varies with depth of the dike. In all cases considered here, the widest total dike opening is at mid-crustal levels. For models that are little affected by heat loss with lithosphere of normal thickness, maximum cumulative dike opening of ~4 km will sufficiently weaken the lithosphere to the point of tectonic rifting (Fig. 5). For very low rates of magma injection, minimum cumulative opening is

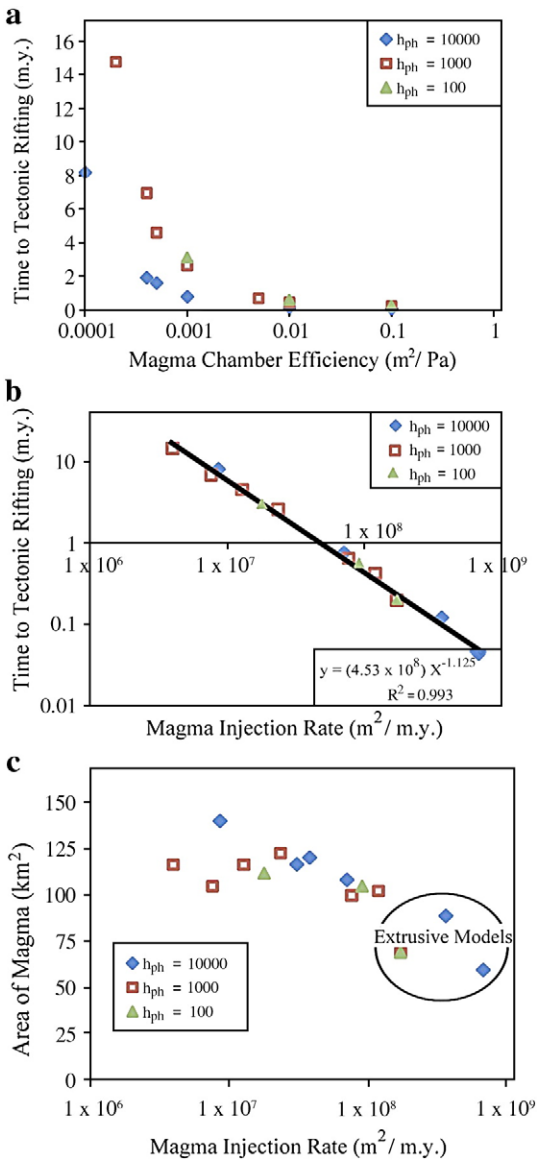

Fig. 7. Model results with $H_L = 80$ km, $F_A = 4.2$ TN m^{-1}. (a) Plot of time versus MCE for varied h_{ph}. Decreasing magma supply or decreasing magma pressure leads to longer time to tectonic rifting. (b) Log–log plot of time to tectonic rifting versus magma injection rate, $\dot{m}$ (m^2 m.y.$^{-1}$). As magma flux decreases, the time to tectonic rifting increases as a power law function. (c) Total area of magma (km^2) at time of transition vs. $\dot{m}$. With increasing time, there is a small increase in the amount of required magma, and less magma is needed in cases where extrusives decrease ΔF.

affected by thermal diffusion. If all heat from a dike is conductively cooled away from the injection zone before the next intrusion, the system will never transition to a tectonic rift. If cooling is not important in the system, then the total volume of magma required to tectonically rift will be independent of $\dot{m}$. For such cases, the slope of a power law function relating $\dot{m}$ and time to tectonic rifting would be −1.

Fig. 8a plots time to tectonic rifting versus $\dot{m}$ for 4 cases: 1. 80 km lithosphere, 40 km crust, and $F_A = 4.2$ TN m^{-1} (the suite of models presented in Fig. 7), 2. 80 km lithosphere, 40 km crust, and $F_A = 2$ TN m^{-1}, 3. 60 km lithosphere, 30 km crust, and $F_A = 2$ TN m^{-1}, and 4. 20 km lithosphere, 6 km crust, $F_A = 1$ TN m^{-1}. Models affected by extrusion are excluded. For models with lithsopheric thickness ≥60 km, the slope of the power law relationship is close to −1, implying minimal cooling. The total required area of magma (Fig. 8b) shows small increases with time for cases with $H_L \geq 60$ km. While more magma is required with lower extensional force (80 km 4 TN m^{-1} vs. 2 TN m^{-1}), the lower force series also only requires a modest increase in magma with time.

For thin lithosphere, diffusion is more important, evidenced by the power law slope for the series with 20 km lithosphere and 6 km crust, which equals −1.8. (Fig. 8a). For this case, the linear rate of increase in the area of magma is ~4 times greater than that of the 60 km series (Fig. 8b). The increased influence of thermal diffusion with thinner lithosphere is related to the initial thermal profile. Isotherms are much closer together in the thin lithosphere and, as a result, are much closer to this surface boundary condition, set to $T(\text{surface}) = 0$ °C. As a result, more heat is lost out of the model domain than for models with thick lithosphere.

6.2. Comparison to other models

Previous models combining a fully visco-elastic-plastic code with simulated dike intrusion have relied on the *M*-factor approximation (e.g. Buck et al., 2005; Tucholke et al., 2008) in which some fraction of extension, the *M*-factor, is accommodated by accreting a set width of hot material onto a vertical column of diking nodes. Our approach has three major advantages over the *M*-factor method. First, in our method, the top, bottom, and width of the dike are calculated as a response to the stress field and prescribed magmatic parameters, where as the *M*-factor approach uses predetermined values for dike dimensions. As demonstrated in our results, the shape of an individual dike changes with depth, thermal structure, and rheology. Second, *M*-factor models assume enough force is present to extend the lithosphere, which we argue is not always true in natural systems. Our model does not stretch the lithosphere when available force is below that necessary to extend. This affects dike shape and magma distribution with depth and time. Lastly, our approach allows extrusion to be treated in a reasonable way based on the size of the dike calculated from the stress field and the available magma supply. *M*-factor models have not treated extrusion. As discussed above, extrusion affects the stress field and can reduce the amount of intruded magma required for tectonic rifting.

Recent work using the *M*-factor approach addressed how much magmatic weakening is required to rift continental lithosphere. For a similar definition of normal lithosphere as used here, Behn et al. (2009) report that ~4 km of dike opening is required to transition to a tectonic rift, similar to our maximum cumulative dike opening. However, the total volume per unit length of magma required by our approach is less than half that predicted by this *M*-factor approach (Figs. 7c and 8b). This difference stems from the changes in magma distribution through space and time, discussed above, allowed in our simulation. This reduction may be significant when considering the influence of magmatism on the evolution of margins traditionally viewed as magma-poor, as the presence of a small amount of pre-rift magmatism, potentially all intrusive, can have a large impact on rift development. However, the similarity in the total width of opening between the two studies is encouraging. *M*-factor models, while making a set of much simpler assumptions, are easier and faster to run and still seem to still provide a reasonable way to simulate some of the effects of repeat dike intrusion.

6.3. How thick is too thick?

Given the force requirements for our velocity boundary condition, our model is well suited to test the maximum thickness of lithosphere that may magmatically rift. Following the analytical model description, the required force to open a dike through the lithosphere is:

$$F_{req} = \int (S_v - P_m) dz \quad (8)$$

Fig. 9a plots the F_{req} for a section of lithosphere with 40 km crust and increasing thickness of mantle lithosphere with $h_{ph} = 1$ km and 100 m.

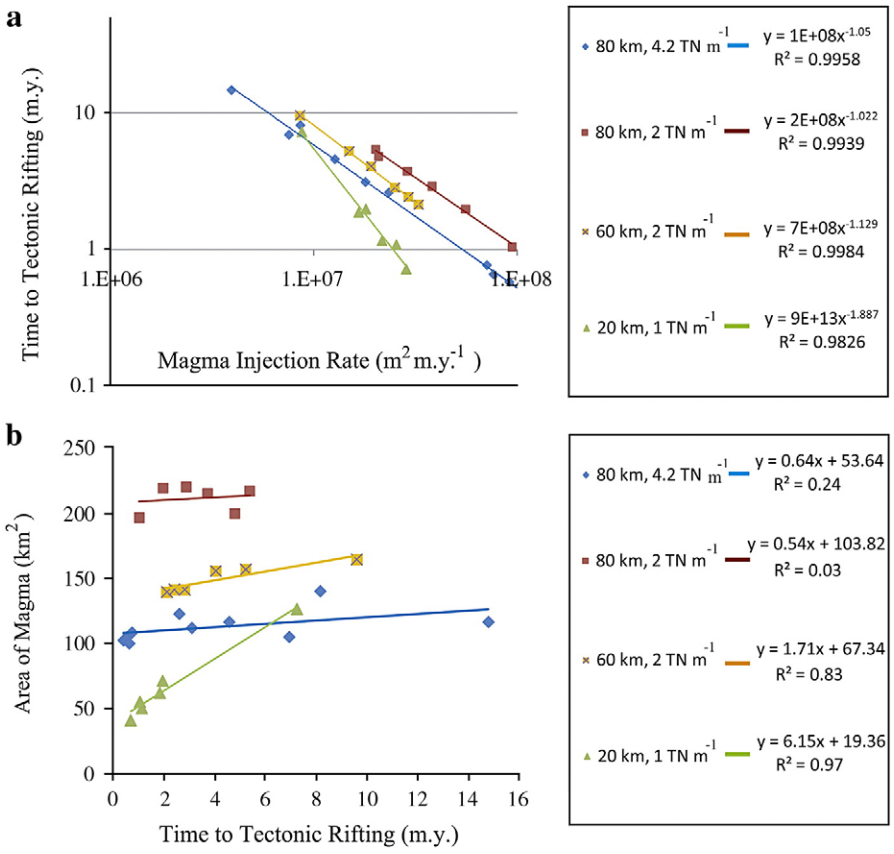

Fig. 8. (a) Log–log plot of time to tectonic rifting versus $\dot{m}$ for 4 series with varying lithospheric thickness and rifting force. Highly extrusive simulations are excluded. The slope of the power law function for series with lithosphere ≥60 km is close to −1, implying the required area of magma to tectonically rift changes little with time, which is confirmed in the area of magma plot in (b). The slope of the 20 km series is −1.9. As predicted, the increase in area of magma with time (b), is 3–4 times larger for the 20 km case than the other cases.

The horizontal red line is the available extensional force, $F_A = 4$ TN m^{-1}. If $F_{req} > F_A$, the lithosphere will not be able to rift. Analytically, the maximum lithospheric thickness into which dikes may intrude is ~80 km for $h_{ph} = 100$ m and ~90 km for $h_{ph} = 1$ km.

Numerically, the solution for the maximum "riftable" lithospheric thickness depends on the magma supply parameters and on the time over which magma is supplied to the rift. Fig. 9b shows the time to tectonic rifting for models with 40 km crust and increasing mantle lithospheric thickness for series with $h_{ph} = 100$ m and 1 km and MCE = 0.01 m^2 Pa^{-1}. The base of the lithosphere is defined here as the thermal lithosphere at the 1200 °C isotherm. As lithospheric thickness approaches its critical value for a set h_{ph}, dikes do not open deep enough to rift the lithosphere and the time to tectonic rifting becomes infinitely long. With higher pressure head, thicker sections of lithosphere may rift, as predicted by the analytical model. The maximum riftable thickness is ~100 km and ~112 km for $h_{ph} = 100$ m and 1 km, respectively. The 20 km difference between numerical and analytical thicknesses arises from the ability of the ductile portion of the mantle lithosphere in numerical models to extend without dike injection. Maximum penetration depth of numerical dikes is ~85 km and 95 km for $h_{ph} = 100$ m and 1 km, respectively, only 5 km larger than the analytical approach. Thus, choosing a lower value of the temperature marking the bases of the lithosphere would bring the analytical and numerical models into closer agreement. For reasonable values of pressure head and moderate extensional force, it is unlikely that extremely thick continental lithosphere (i.e. well over 100 km) would be able to magmatically rift.

6.4. Implications for real rifts

We find that for moderate rift opening times (from a few to a few 10's of Ma) the amount of total magma needed to cause sufficient lithospheric weakening depends mainly on the initial lithospheric thickness. With thicker mantle lithosphere more magma is required not only due to the thickness increase but also because of the lower thermal gradient compared to thinner lithosphere models. In this paper we define lithosphere in terms of the depth to a set isotherm (1200 °C). However, at the rates of deformation considered here, we only see brittle behavior down to about the 1000 °C isotherm in the mantle. Because our idealized models do not consider heat-producing elements in the crust, it is difficult to directly compare our results to natural systems where surface heat flow is the primary constraint on the lithospheric structure. Heat-producing elements would increase temperatures in the crust and upper mantle, making for a higher surface heat flow for a similar thickness of lithosphere. Our results, therefore, over-estimate the amount of magma needed to sufficiently weaken the lithosphere with a given surface heat flow.

Our results have bearing on many natural rift systems. By changing the diking parameters, our models can simulate the behavior of different magmatic rifts. Highly extrusive models with fast transitions to tectonic rifting match the behavior of rifts initiated contemporaneously with or immediately after emplacement of seaward dipping reflectors, such as the Greenland Margin (Hopper et al., 2003) or South Atlantic (Gladczenko et al., 1997). Largely intrusive models with longer transitions may match the early history of the East African Rift and Red Sea (Keranen et al., 2004; Kendall et al., 2005). Our models demonstrate that some non-volcanic rifts could have been significantly weakened by relatively small amounts of intruded magma.

It is difficult to constrain how fast magma is intruded into natural magmatic rifts. However, the observed rate of magma extrusion in large igneous provinces is similar to the intrusion fluxes needed to significantly weaken our model rifts. Courtillot and Renne (2003) report an average flux for LIPs to be ~2 km^3 yr^{-1}. If such a flux were

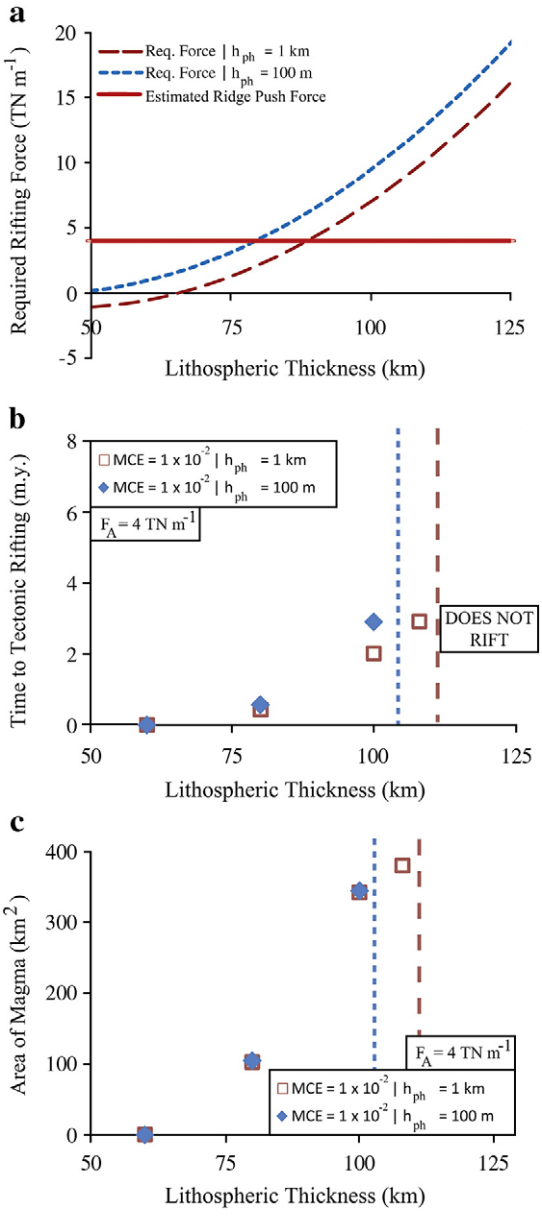

Fig. 9. (a) Plot of the analytical solution for the force required to open a dike the height of the lithosphere versus lithospheric thickness for $h_{ph}=100$ m and 1 km. A red line is drawn at 4 TN m^{-1}, the available rifting force (~ridge push) in the numerical models. Negative force means that no additional tectonic force is required to rift. (b) The time to tectonic rifting versus lithospheric thickness for numerical models with a MCE $=10^{-2}$ m^2 Pa^{-1}, $h_{ph}=100$ m and 1 km, and $F_A=4$ TN m^{-1}. Blue and red dashed lines indicate the maximum riftable thickness of lithosphere for $h_{ph}=100$ m and 1 km, respectively, constrained by additional models in which dikes were unable to penetrate the whole brittle portion of the lithosphere. With increasing lithospheric thickness, the time to tectonic rifting increases until the system cannot rift. Numerical maximum riftable lithospheric thickness is ~100 km and ~112 km for $h_{ph}=100$ m and 1 km, respectively. (c) Plot of the area of magma required to transition to tectonic rift versus lithospheric thickness.

intruded along a 2000 km long rift, the implied intrusion rate would be 10^9 m^2 $m.y.^{-1}$, comparable to our highest flux cases. In addition, dikes >10 m wide, similar to those developed in our numerical models with high to medium $\dot{m}$, are observed in continental rifts associated with LIPs (Fahrig, 1987). We therefore believe our highest values of $\dot{m}$ to be reasonable.

The amount of magma needed for complete rifting is reasonable. For every 1000 km of rift cutting normal continental lithosphere (defined here as having ~30 km of brittle mantle lithosphere) we expect that ~10^5 km^3 of basalt (~100 km^2 of magma for 80 km thick lithosphere by 1000 km length of rift) would be needed to weaken the rift to allow tectonic stretching at reasonable force levels. Even for the 2000 km long Red Sea rift, the amount of magma required is less than two-thirds the estimated 3.5×105 km^3 of basalt present today, post erosion, on the Ethiopian and Yemen Plateau at 30 Ma (Mohr, 1983). Thus, a fraction of the magma produced in short-lived volcanic pulses associated with LIPs could be enough to initiate a rift in moderately old continental lithosphere.

7. Conclusions

Our modeling approach, which calculates dike opening in terms of the stress distribution before and after the dike intrusion for set parameters controlling the available magma supply and pressure, allows us to investigate the amount of magma required to transition a section of continental lithosphere from a magmatically assisted rift to a tectonic rift. For an 80 km thick section of continental lithosphere, the amount of magma needed is small; maximum cumulative dike opening is ~4 km in the mid- to upper crust, with substantially less opening in the hotter mantle regions. The total volume of magma required by this approach is roughly half that of previous studies which assumed uniform dike width with depth. The time required for this transition decreases almost linearly with the inverse of the magma injection rate. For thick lithosphere, ≥60 km, the amount of magma is little affected by thermal diffusion. Thinner lithosphere is more affected by heat loss, and the transition requires more cumulative dike opening. In addition, we observe that large volumes of extrusives can influence the available rifting force and transition rifts to tectonic rifting earlier than expected.

Increasing magma pressure head allows thicker sections of lithosphere to magmatically rift. Numerical results for the maximum riftable thickness agree with our analytical estimate. Very thick continental lithosphere, >100 km, probably cannot rift under conditions found on Earth.

Changes in magmatic input can produce a range of rift types comparable to those observed in nature, from slightly magmatic rifts to highly volcanic rifts.

Acknowledgements

Thank you to NSF OCE 05-48877, NSF EAR 06-35898, and NSF OCE 04-26575 for funding this work, Donna Shillington for her helpful suggestions, and Eunseo Choi, Trish Gregg, and Mark Behn for their helpful discussions.

Appendix A. Calculating dike opening

We use an iterative process to calculate a dike top, bottom, and dike width at depth which balances the pressure in the dike wall derived from the injected magma and the pressure on the dike wall from the local stress field. For each dike event, an initial test "seed" depth is set, and the top and bottom of the dike are moved away from the seed as long as the boundary element calculation for an iteration indicates opening at those points. For our 80 km thick lithosphere cases, we use the depth of the 700 °C isotherm as our seed depth, ~50–60 km. For thicker models, we keep the seed depth at 50–60 km, tying it to the appropriate isotherm. Altering the seed point position can change the magma injection history. If dikes are inputted at shallow levels and breach the surface, they will not penetrate as deep as dikes with deeper seed points. Initial dike size is small, usually 1–2 km. Initial dike size is important for opening and growing of the initial dike, but in cases where dikes will open, the final dike size of an event is not affected by the initial dike size.

Pressure in the dike wall is solved for during each iteration in terms of pressure head above the top of the dike, referred to as the

magma top. Given an initial guess for the magma top, dike opening is calculated by balancing the stress field and magma pressure. After dike opening is calculated, we compare the volume per unit length of the injected magma with that of the available magma supply:

$$\int \Delta x(z)dz \text{ vs. } \left(h_{ph} - \text{dike top} - \text{magma top}\right) * \rho_m * g * \text{MCE}$$

where $\Delta x(z)$ is the dike width with depth. If the volume of injected magma is not within 10% of the available magma supply, we increase or decrease the magma top accordingly.

Once a magma top has been established, we again check the opening at the top and bottom of the dike. If the opening is larger than 0.1 m (for the H_L range explored in this paper), the dike top (or bottom) is increased, increasing the dike height. If there is negative opening at either dike tip, the dike height is reduced by adjusting the dike top or bottom accordingly.

References

Behn, M.D., Buck, W.R., Bialas, R.W., 2009. The influence of magmatism on rift initiation. Eos Trans. AGU 90 (52) Fall Meet. Suppl., Abstract T24D-05.

Bialas, R.W., Buck, W.R., Studinger, M., Fitzgerald, P.G., 2007. Plateau collapse model for the Transantarctic Mountains–West Antarctic Rift System: insights from numerical experiments. Geology 35 (687–690).

Bosworth, W., Huchon, P., McClay, K., 2005. The Red Sea and Gulf of Aden Basins. J. Afr. Earth Sci. 43, 334–378.

Bott, M.H.P., 1991. Ridge push and associated plate interior stress in normal and hot spot regions. Tectonophysics 200, 17–32.

Braun, J., Beaumont, C., 1989. A physical explanation of the relation between flank uplifts and the breakup unconformity at rifted continental margins. Geology 17, 760–764.

Buck, W.R., 1991. Modes of continental lithospheric extension. J. Geophys. Res., B, Solid Earth Planets 96 (12), 20,161–120,178.

Buck, W.R., 2004. Consequences of asthenospheric variability on continental rifting. In: Karner, G.D., Taylor, B., Driscoll, N.W., Kohlstedt, D.L. (Eds.), Rheology and Deformation of the Lithosphere at Continental Margins. Columbia University Press, New York, pp. 1–31.

Buck, W.R., 2006. The role of magma in the development of the Afro–Arabian Rift System. In: Yirgu, G., Ebinger, C.J., Maguire, P.K.H. (Eds.), The Afar Volcanic Province within the East African Rift System. : Special Publications. Geological Society of London, London, pp. 43–54.

Buck, W.R., Lavier, L.L., Poliakov, A.N.B., 2005. Modes of faulting at mid-ocean ridges. Nature 434, 719–723.

Coltice, N., Bertrand, H., Rey, P., Jourdan, F., Phillips, B., Ricard, Y., 2009. Global warming of the mantle beneath continents back to the Archaean. Gondwana Research 15, 254–266.

Courtillot, V.E., Renne, P.R., 2003. On the ages of flood basalt events. In: Courtillot, V.E. (Ed.), The Earth's Dynamics: Comptes Rendus - Academie des Sciences, pp. 113–140.

Courtillot, V.E., Jaupart, C., Manighetti, I., Tapponnier, P., Besse, J., 1999. On the casual links between flood basalts and continental breakup. Earth Planet. Sci. Lett. 166 (177–195).

Crouch, A.L., Starfield, A.M., 1983. Boundary Element Methods in Solid Mechanics. George Allen and Unwin, London.

Cundall, P.A., 1989. Numerical experiments on localization in frictional materials. Ingenieur Archiv. 58, 148–159.

Davis, M., Kusznir, N., 2004. Depth dependent lithospheric stretching at rifted continental margins. In: Karner, C.S. (Ed.), Rheology and Deformation of the Earth's Lithosphere at Continental Margins. Columbia University Press, New York, pp. 92–137.

Einarsson, P., 1991. The Krafla rifting episode 1975–1989. In: A.E., Gardarsson, A. (Eds.), Na´ttu´ra M'yvatns, (The Nature of Lake M'yvatn). Icelandic Nature Science Society, Reykjavik, pp. 97–139.

Ernst, R.E., Buchan, K.L., 1997. Giant radiating dyke swarms: their use in identifying pre-Mesozoic large igneous provinces and mantle plumes. In: Mahoney, J.J., Coffin, M.F. (Eds.), Large Igneous Provinces: Continental, Oceanic, and Planetary Flood Volcanism. AGU, Washington, D.C., pp. 297–334.

Fahrig, W.F., 1987. The tectonic setting of continental mafic dyke swarms: failed arm and early passive margin. In: Halls, H.C., Fahrig, W.F. (Eds.), Mafic Dyke Swarms: Geological Association of Canada Special Paper, pp. 331–348.

Fialko, A.Y., Rubin, A.M., 1999. Thermal and mechanical aspects of magma emplacement in giant dike swarms. J. Geophys. Res. 104 (B10), 23,033–023,049.

Gladczenko, T.P., Hinz, K., Eldholm, O., Meyer, H., Neben, S., Skogseid, J., 1997. South Atlantic volcanic margins. J. Geol. Soc. 154, 465–470.

Hill, R.I., 1991. Starting plumes and continental breakup. Earth Planet. Sci. Lett. 104, 398–416.

Hinz, K., 1981. A hypothesis on terrestial catastrophes wedges of very thick oceanward dipping layers beaneath passive margins. Geol. Jahrb. 22, 5–28.

Hopper, J.R., Dahl-Jensen, T., Holbrook, W.S., Larsen, H.C., Lizarralde, D., Korenaga, J., Kend, G.M., Kelemen, P.B., 2003. Structure of the SE Greenland margin from seismic reflection and refraction data: implications for nascent spreading center subsidence and asymmetric crustal accretion during North Atlantic opening. J. Geophys. Res. 108 (B5).

Kendall, J.M., Stuart, G.W., Ebinger, C.J., Bastow, I.D., Keir, D., 2005. Magma-assisted rifting in Ethiopia. Nature 433, 146–148.

Keranen, K., Klemperer, S.L., Gloaguen, R., EAGLE Working Group, 2004. Three-dimensional seismic imagining of a protoridge axis in the Main Ethiopian rift. Geology 32, 949–952.

Kirby, S.H., Kronenberg, A.K., 1987. Rheology of the lithosphere: selected topics. Rev. Geophys. 25, 1219–1244.

Lavier, L., et al., 2000. Factors controlling normal fault offset in an ideal brittle layer. J. Geophys. Res. 105 (B10), 23431–23442.

LeCheminant, A.N., Heaman, K.M., 1989. McKenzie igneous events, Canada: Middle Proterozoic hotspot magmatism associated with ocean opening. Earth Planet. Sci. Lett. 96, 38–48.

McKenzie, D., 1978. Some remarks on the development of sedimentary basins. Earth Planet. Sci. Lett. 40, 25–32.

Mogi, K., 1958. Relations of eruptions of various volcanoes and the deformation of the ground surfaces around them. Bull. Earthquake Res. Inst. Univ. Tokyo 39, 99–134.

Mohr, P., 1983. Ethiopian flood basalt province. Nature 303, 577–584.

NieIsen, T.K., Hopper, J.R., 2002. Formation of volcanic rifted margins: are temperature anomalies required? Geophys. Res. Lett. 2910.1029/2002GL015681.

Qin, R., 2008. Mid-ocean ridge morphology and tectonics: insights from numerical modeling of faults and dikes, PhD, Columbia University, New York.

Qin, R., Buck, W.R., 2008. Why meter-wide dikes at oceanic spreading centers? Earth Planet. Sci. Lett. 265, 466–474.

Royden, L., Keen, C.E., 1980. Rifting process and thermal evolution of the continental margin of eastern Canada determined from subsidence curves. Earth Planet. Sci. Lett. 51, 343–361.

Royden, L., Sclater, J.G., Von Herzen, R.P., 1980. Continental margin subsidence and heat flow: important parameters in formation of petroleum hydrocarbons. Bull. Am. Assoc. Pet. Geol. 64, 173–187.

Rubin, A.M., 1990. A comparison of rift-zone tectonics in Iceland and Hawaii. Bull. Volcanol. 52, 302–319.

Rubin, A.M., Pollard, D.D., 1987. Origins of Blake-Like Dikes in Volcanic Rift Zones, 1449–1470 pp, U.S. Geological Survey Professional Paper 1350.

Saemundsson, K., 1979. Fissure swarms and central volcanoes of the neovolcanic zones of Iceland. Geol. J. 19, 415–432.

Segall, P., Cervelli, S., Owen, S., Lisowski, M., Miklus, A., 2001. Constraints on dike propagation from continuous GPS measurements. J. Geophys. Res. 106, 19,301–319,318.

Spohn, T., Schubert, G., 1982. Convective thinning of the lithosphere; a mechanism for this initiation of continental rifting. J. Geophys. Res. 87, 4669–4681.

Tryggvason, E., 1984. Widening of the Krafla fissure swarm during the 1975–1981 volcano-tectonic episode. Bull. Volcanol. 47 (1), 47–69.

Tucholke, B.E., Behn, M.D., Buck, W.R., Lin, J., 2008. Role of melt supply in oceanic detachment faulting and formation of magamullions. Geology 36, 455–458.

Turcotte, D., Schubert, G., 2002. Geodynamics. Cambridge University Press, New York.

van Wijk, J.W., Huismans, R.S., ter Voorde, M., Cloetingh, S.A.P.L., 2001. Melt generation at volcanic continental margins: no need for a mantle plume? Geophys. Res. Lett. 28 (20), 3995–3998.

Weertman, J., 1971. Theory of water-filled crevasses in glaciers applied to vertical magma transport beneath oceanic ridges. J. Geophys. Res. 76 (5), 1171–1183.

White, R., McKenzie, D., 1989. Magmatism at rift zones: the generation of volcanic continental margins and flood basalts. J. Geophys. Res. 94, 7685–7729.

Wolfenden, E., Ebinger, C., Yirgu, G., Deino, A., Ayalew, D., 2004. Evolution of the northern Main Ethiopian rift: birth of a triple junction. Earth Planet. Sci. Lett. 224, 213–228.

Wolfenden, E., Ebinger, C., Yirgu, G., Renne, P., Kelley, S., 2005. Evolution of a volcanic rifted margin: Southern Red Sea, Ethiopia. GSA Bull. 117 (7/8), 846–864.